Soft Matter

Accepted Manuscript

ROYAL SOCIETY OF CHEMISTRY

www.rsc.org/softmatter

Cite this: DOI: 10.1039/c0xx00000x

www.rsc.org/xxxxxx

ARTICLE TYPE

Lipid directed assembly of the HIV capsid protein

Penny Miles[a] and Daniel Frankel*[a]

Received (in XXX, XXX) Xth XXXXXXXXX 20XX, Accepted Xth XXXXXXXXX 20XX
DOI: 10.1039/b000000x

Experimental evidence for *in-vivo* capsid assembly suggests that capsid formation initiates from interactions between capsid (CA) proteins and lipids in the viral envelope. Various *in-vitro* studies aiming to elucidate the detailed mechanisms of capsid self-assembly products have been carried out in conditions far removed from those, which would be encountered in a physiological environment. In this work we used lipid bilayers as a platform for studying the assembly of the CA protein with the rationale that the lipid-CA interactions play an important role in the nucleation of these structures. Observations using atomic force microscopy (AFM) have allowed a 'curling tadpole' mechanism to be suggested for the capsid self-assembly process. Stable dimeric CA proteins are able to move across the lipid bilayer to associate into trimers-of-dimers. These trimers form distinctly curved chains, which coil up to form larger features. As the feature grows additional trimers associate with the feature, giving a tadpole-like appearance. By comparing capsid assembly on mica, on single component lipid bilayers, and phase separated lipid bilayers, it was possible to determine the effect of lipid-protein interactions on capsid assembly.

Introduction

HIV infection is the causative agent of AIDS [1], the treatment of which relies heavily on the use of antiretroviral drugs. However, the HIV virus, unlike prokaryotic and eukaryotic cells, does not have a proofreading mechanism, therefore errors in transcription and translation of the genetic material are common and result in mutations [2, 3]. The majority of these mutations lead to the assembly of non-functional proteins, but in some cases the mutation is advantageous and results in the virus becoming resistance to anti-retroviral drugs [4]. Therefore new and innovative therapies must be continuously developed to treat this infection [5]. Antiretroviral therapies which target the capsid may provide a new avenue in the treatment of AIDS/HIV as the capsid protein exhibits high sequence conservation levels and many single point mutations result in decreased replication efficiency [6]. Knowledge of the mechanism by which capsid proteins assemble in an *in-vitro* environment may prove crucial to the development of these drugs.

The human immunodeficiency virus (HIV) assembles and buds from an infected host cell as an immature virion with a layer of Gag polyproteins bound to the inner viral lipid envelope [6, 7]. Gag polyproteins consist of a number of protein domains, including the capsid protein (CA, p24), which are separated by enzymatic cleavage as the virus matures [5, 8]. During maturation, the Gag hexagonal lattice rearranges into a number of structures, one of these structures is the conical viral capsid which contains the dimeric RNA and is responsible for RNA organisation within a new host cell [7, 9, 10]. Whilst the structures of both the mature and immature virus particles are well understood, the assembly pathway between the two is unclear.

To date a number of studies have investigated the *in-vitro* self-assembly products of CA using techniques such as electron microscopy (EM), florescence microscopy (FM) and gel electrophoresis [11-15]. The use of Atomic force microscopy (AFM) in this paper facilitates the study of protein self-assembly in a more biologically relevant environment (under liquid buffer conditions as opposed to the vacuum required for EM) and is able to achieve nanoscale resolution in the z-direction. The use of supported lipid bilayers provide a biomimetic environment in which to investigate the fundamental interactions of proteins and their self-assembly behaviour.

CA has been shown to consist of two independently folded domains joined by a flexible linkage [16-19]. The molecular dimensions of which have been determined by x-ray crystallography and are important measures when using size considerations to assign molecular scale features during self-assembly [16-18]. The CA protein self-associates in solution to form oligomers of various sizes, however dimers have been found to be the most stable complex formed [14, 20]. Following cleavage of the Gag polyprotein, the mature HIV capsid assembles from approximately 1,500 CA proteins into a fullerene cone structure [21, 22]. Electron microscopy has shown that the conical capsid comprises of primarily hexameric CA oligomers with a small number of pentameric defects allowing a large, enclosed hexagonal surface lattice to be formed [19, 23]. This mature *in-vivo* capsid measures 120 to 130 nm in length, 55 to 62 nm in diameter at the broad end and 25 nm in diameter on the narrow end [20].CA readily self-assembles *in-vitro* into tubular structures under high salt concentrations (greater than 1M NaCl) and low protein

concentrations. At low salt concentrations there are no structures formed [12, 15, 20, 24]. Within mature HIV virions both conical and tubular capsids have been observed at a ratio of 20:1[25]. Tubular capsids were hypothesised to be an intermediate in the formation of the conical capsid. Although tubular structures are found *in-vivo*, the *in-vitro* conditions under which they are formed do not appear to represent a physiologically relevant environment. During virus maturation the core is a crowded environment, formation of the mature capsid requires only a fraction of the available CA molecules [10]. Additionally the other structural proteins present as a result of cleaving the Gag polypeptide effectively increase the concentration of CA present in the core [14]. Natural and synthetic polymers, known as crowding agents, mimic the crowded environment within the viral core and promote the formation of tubular capsid structures, under physiological salt conditions [13]. However, these inert natural and synthetic polymers are not representative of the molecules present in the viral core during maturation.

Capsid assembly has been proposed to proceed in a similar manner both *in-vivo* and *in-vitro*, with different final structures forming [26]. This assembly mechanism suggested that the capsid, nucleocapsid (NC) and RNA were all required for capsid formation. RNA plays a key role in the organisation of the assembly process, essentially acting as a template. CA-NC complexes would bind to RNA and then wind up to produce a larger capsid structure, the growth of the structure would continue due to the addition of individual CA-NC complexes or complexes bound to smaller RNAs. More recently individual assembly mechanisms have been proposed. Unlike the previous mechanism these suggest that self-assembly of the capsid structure and its organisation is an inherent property of the capsid protein. *In-vivo*, capsid formation initiates from the narrow end of the structure, with the initial CA proteins being tethered to the viral lipid envelope. Capsid growth then proceeds towards the opposite side of the virion where the broad end is formed due to interactions with either the matrix or viral envelope [27]. Interactions between CA and lipids therefore play a key role in the initiation of capsid formation.

Barklis et al. proposed that *in-vitro*, tubular capsid self-assembly consists of a rate-limiting nucleation stage followed by a rapid growth period in which the complexes are able to extend in either direction [12]. However In their study, the size of the nucleation complexes was not determined due to limitations of the available resolution of the EM and fluorescence techniques employed. Mathematical modelling investigating the early-stages of the capsid assembly process potentially sheds light on the size of the initial nucleation complexes [28]. CA proteins are known to readily dimerise in solution [20], these initial dimers associate to form 'trimers-of-dimers' which are crucial in the production of the hexagonal CA lattice of the capsid structure [28]. The *in-vivo* model of capsid assembly suggests that the viral envelope plays a key role in the nucleation process, therefore in this paper the work focuses on examining capsid self-assembly in the presence of lipids. Whilst there are numerous studies of the self-assembly products of capsid proteins, there is still a large amount of understanding to be gained of the assembly process. The model of a rate-limiting nucleation period followed by a rapid growth period is currently the accepted description. The key issues with this model are the conditions under which it was developed and the number of unknowns which remain. The growth period was assumed to be rapid due to the fact that a large number of tubular structures were observed, this could primarily be due to the resolution of the EM and FM not revealing an abundance of nucleation complexes present.

AFM is a non-destructive high-resolution technique which as well as producing nanoscale resolution in the x, y and z directions, allows the mechanical properties of the self-assembled structures to be probed using single molecule force spectroscopy (SMFS). A particular advantage over electron microscopy is that the assembly process of biomolecules can be examined in a liquid environment. Supported lipid bilayers are an ideal platform to measure the physical/chemical interactions of biomolecules with lipids as they present chemical lipid head groups and packing whilst being flat enough to allow interrogation by high-resolution techniques such as AFM.

Materials and Methods

Supported lipid bilayer preparation

1,2-dioleoyl-sn-glycero-3-phosphocholine (DOPC) and 1,2-dipalmitoyl-sn-glycero-3-phosphocholine (DPPC) (Avanti Polar Lipids) were dissolved in chloroform and the solvent removed under a nitrogen flow. The lipids were re-suspended in purified water and mixed to give a 1mg/mL aqueous suspension. Ten freeze/thaw cycles were carried out, followed by eleven extrusion cycles at 45°C using a mini extruder (Avanti Polar Lipids) with a 50nm polycarbonate membrane to yield a homogenous mixture of unilamellar lipid vesicles. Supported lipid bilayers were prepared by the process of vesicle fusion. 400µL of vesicle solution was deposited onto freshly cleaved mica and incubated for 20 minutes at 45°C. Prior to imaging the bilayer was washed three times with phosphate buffered saline (PBS) solution.

CA protein adsorption

Aliquots of recombinant HIV p24 full-length protein (ab49055, Abcam) were diluted in purified water to a concentration of 2 µg/mL and stored at -20°C. Protein was adsorbed onto a mica surface or supported lipid bilayers, either DOPC or DOPC/DPPC, for 60 minutes. Prior to imaging, the surface was washed three times with PBS solution to remove any un-adsorbed protein.

Topographic AFM imaging

AFM experiments were performed in a liquid cell using an Agilent 5500 AFM/SPM microscope operated using Picoview 1.14 software. Images were obtained in both contact and tapping mode. Nitrogen doped silicon tips (Nanosensors, PPP-CONTR-50) with a nominal force constant of 0.02-0.77N/m were used for contact mode imaging. Nitrogen doped silicon tips (Nanosensors, PPP-NCSTR-50) with a resonance frequency of approximately 84Hz were using for tapping mode imaging. All measurements were performed at ambient temperature and in PBS solution. All image processing was carried out using Scanning Probe Image Processor (SPIP) version 6.1.8 software (Image Metrology, Lyngby, Denmark).

Force spectroscopy

Force spectroscopy experiments were carried out using a gold coated contact mode tip (Budget Sensors, CONT-G) with a nominal force constant of 0.2N/m. The spring constants were determined using equipartition theory (Thermal K). At least 1000 curves were obtained per sample with an applied load in the range 7-10 nm, a constant tip velocity of les than 1 µms-1, and a curve length of up to 1 µm. Curves were analysed using Scanning Probe Image Processor (SPIP) version 6.1.8. (Image Metrology, Lyngby, Denmark). Detachment forces were obtained from the force distance curves and only those curves that could be fitted to the worm like chain model were accepted as representing single molecule binding between the functionalised tip and surface. The tip was functionalised with CA protein by immersing the tip in 100 µg/ml solution of the CA protein for 1 hour. After this period the tip was rinsed three times in PBS buffer. Successful functionalisation was confirmed by measuring force distance curves on mica, the presence of attached protein indicated by a saw tooth pattern on tip retraction from the surface.

Results and Discussion

CA was first examined adsorbed onto freshly cleaved mica in order to follow assembly behaviour in the absence of lipids. Mica is atomically flat over large areas, as shown in the image before protein adsorption (Fig. 1A) and is thus an ideal substrate for imaging single molecules. When adsorbed at a concentration of 2 µg/mL both single molecules and oligomers of CA were observed (Fig. 1B). The average height of the CA features is 2.09 ± 0.06 nm with the range of heights (Fig. 1C) suggesting that CA complexes adsorb to the mica surface in various orientations. CA has been shown to preferentially form dimers and multimers [20], however under perturbations the larger multimeric structures dissociate. Therefore it is proposed that the dimeric structures, which are present on the mica surface, were present in solution prior to protein deposition on the mica surface even though the solution had been well mixed. When monitored over time, there was no significant change in the observed features sizes. This could be due to a number of factors. Firstly non-covalent bonds will have formed between the CA and mica surface preventing aggregation of molecules or causing a structural change in the protein. When DNA is adsorbed onto mica its structure changes such that it lies flat on the substrate surface [29], therefore a similar conformational change may occur when CA is adsorbed. Secondly *in-vitro* capsid assembly requires high salt concentration or crowding agents to be present, therefore the low salt concentration (0.1M) in the PBS buffer and mica surface do not promote capsid formation.

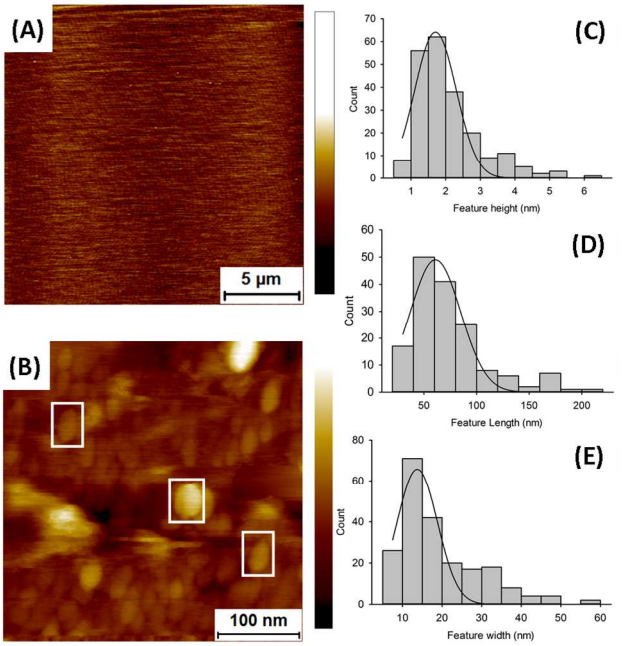

Fig 1. Analysis of CA protein adsorption on bare mica. AFM image of mica before, height scale bar ranging from -0.4 nm (bottom/darkest) to 0.8 nm (top/brightest) (A) and following CA adsorption, height scale bar ranging from -2.5 nm (bottom/darkest) to 7.5 nm (top/brightest) (B). Distribution histograms of feature heights (C), lengths (D) and widths (E). The average heights, lengths and widths were found to be 2.09 ± 0.06 nm (mean = 2.09; SD = 0.95; n = 215), 73.4 ± 2.80 nm (mean = 73.4; SD = 35.2; n = 158), and 19.5 ± 0.69 nm (mean = 19.5; SD = 10.1; n = 228), respectively.

The *in-vivo* mechanism for capsid assembly suggests that the initial nucleation CA proteins are tethered to the viral envelope [27]. In order to more closely mimic this environment supported single phase DOPC lipid bilayers were formed onto which 2 µg/mL of protein was adsorbed and imaged under PBS buffer conditions using the AFM. The DOPC bilayer appears as a flat surface (Fig. 2A). Following protein deposition a number of features were immediately observed (Fig. 2B), from single molecules to chains and aggregates. Aggregates appeared to form 'tadpole'-like features with a large head connected to, or in close proximity to, a chain of CA molecules. One of these features (Fig. 2C) is followed over a 20 minute period. The head was found to increase in both length and width, additionally, the tail length also increased over time (Table 1). This 'tadpole' feature appears to be a significant stage in the self-assembly process with both large and smaller features being observed to have tails which coil up to increase the size of the main structure. On mica, these tadpole features were not observed. There are two proposed explanations for the difference in these results. Firstly DOPC is in the fluid phase at room temperature so it facilitates the movement of CA and therefore oligomerisation, i.e. it has the same effect as having the CA proteins in solution. Secondly it could be possible that the interaction between the DOPC lipids and CA proteins initiates the growth of structures. This could depend on charge density emanating from the lipid head groups for example.

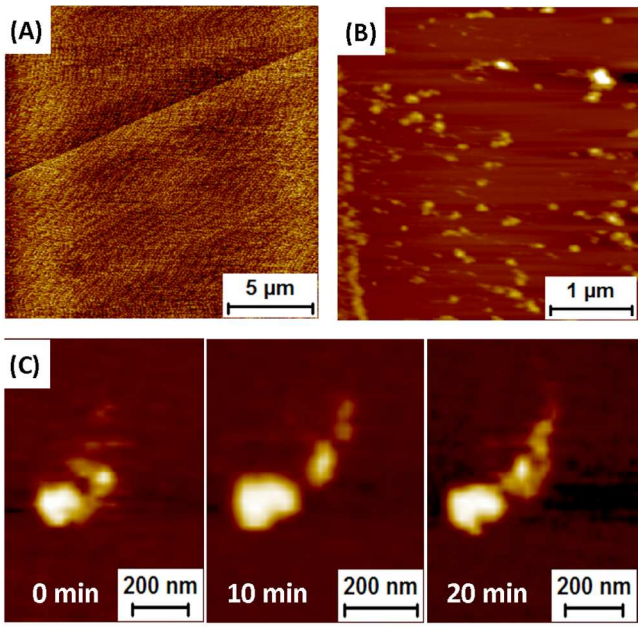

Fig 2. Analysis of CA self-assembly on a single phase bilayer. AFM image of a DOPC bilayer before (A) and after adsorption of 2 µg/mL CA for 60 minutes (B). A 'tadpole' feature was monitored over a period of 20 minutes to observe time-based structural changes (C).

Analysis of the observed features (Fig. 4A-C) shows a bi-modal distribution of structure sizes. The chains of molecules are both smaller in height and width, than the larger tadpole growth complexes. However, the lengths of these two types of structures are similar; this is likely to be due to the fact that as the tadpoles increase in size they coil up, thus getting taller and wider.

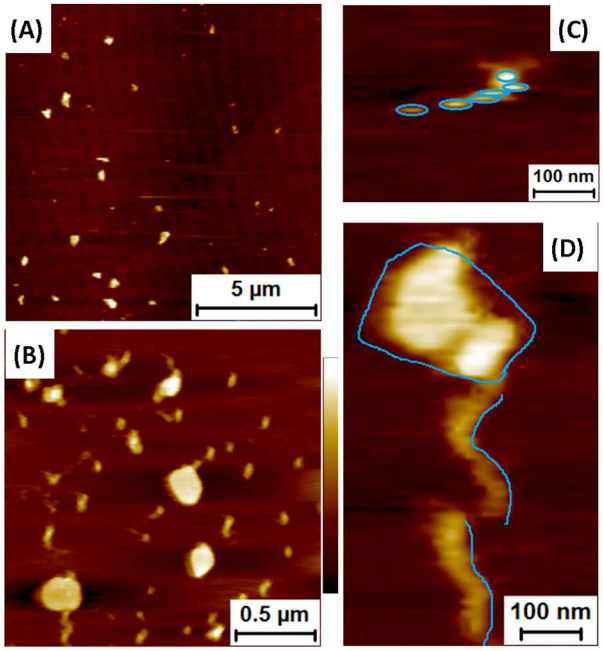

Fig 3. Analysis of CA self-assembly on a phase separated mixed lipid bilayer. AFM image of a DOPC: DPPC bilayer before (A) and 24 hours after adsorption of 2 µg/mL CA protein, height scale bar ranging from -2 nm (bottom/darkest) to 6 nm (top/brightest) (B), both smaller nucleation and larger growth complexes can be seen. A zoom-in of a nucleation complex (C) shows the individual CA molecules coming together and starting to coil to form a 'head' region. Once the head region is established, nucleation 'tails' adds to this in order to increase the structure size (D).

The viral envelope is derived from the host cell membrane and will consist of a diverse range of lipids [30, 31]. Therefore the complexity of the model system was increased by the incorporation of an additional lipid. Phase separated supported lipid bilayers were created using a 3:1 molar ratio of DOPC: DPPC. DPPC is in the gel phase at room temperature and therefore forms distinct domains when a bilayer is formed on mica (Fig. 3A), which measures an average of 1.17 ± 0.03 nm in height. When CA was adsorbed at a concentration of 2 µg/mL, the gel phase microdomains are no longer visible and they are replaced by features of a more distinct morphology, with an average height of 4.51 ± 0.08 nm (Fig. 3B). Analysis of feature heights and profiles confirm that the DPPC domains have disappeared (Fig. 4D). A possible explanation is that interdigitation of the DPPC lipids may have occurred or the adsorption of protein may have caused a physical change in the DPPC domain, i.e. they become fluid. On the mixed bilayer, a number of visually distinct complexes can be seen, dimers, which measure 84.5 ± 2.13 nm in length and 50.0 ± 0.61 nm in width, trimer-of-dimers, chains of molecules measuring 245 ± 9.86 nm, approximately three times the length of a dimer, and larger growth complexes. It is thus possible to observe multiple features of the various stages of capsid formation within the same image, allowing the mode of assembly to be deduced.

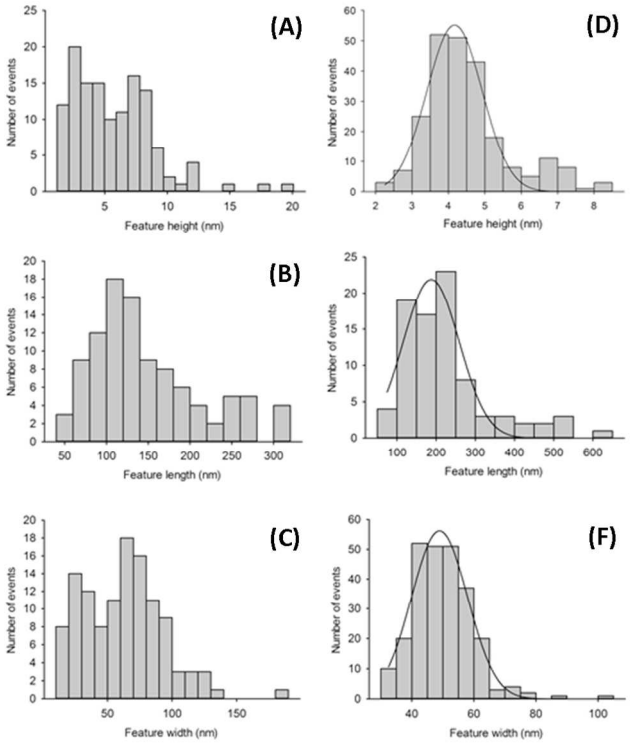

Fig 4. Size data comparison of CA self-assembly products on single phase and mixed lipid bilayers. Distribution of the nucleation and larger growth complex heights, lengths and widths on a single DOPC bilayer are given in (A), (B), and (C). The average heights, lengths and widths were found to be 5.76 ± 0.28 nm (mean = 5.76; SD = 3.22; n = 129), 147 ± 6.50 nm (mean = 147; SD = 65.4; n = 101), and 62.6 ± 2.85 nm (mean = 62.6; SD = 31.1; n = 118), respectively. Distribution of the nucleation complex heights, lengths and widths on a mixed DOPC: DPPC bilayer are given in

(D), (E), and (F). The average heights, lengths and widths were found to be 4.51 ± 0.08 nm (mean = 4.51; SD = 1.16; n = 235), 127 ± 4.59 nm (mean = 127; SD = 70.5; n = 236), and 50.0 ± 0.61 nm (mean = 50.0; SD = 9.62; n = 252), respectively.

A comparison with the measurement of a single CA protein as observed under AFM reveals that the dimer is more compact than the sum of its parts. This can be attributed to the method by which the CA molecules bind together and the finding is analogous to previous studies which have shown that the CA hexamers are more compact than expected based upon the sizes of the individual components[32]. The trimers-of-dimers are not compacted, suggesting a different type of bonding between the dimers compared with the individual molecules. Many of the growth complexes observed can again be described to look like tadpoles with a main feature, the head, connected to a trimer, the tail. In some cases the tail is seen to have almost been incorporated into the main feature. The trimers have a characteristic curvature (Fig. 3C-D), which appears to facilitate the coiling of the chains as they are added to the larger growth complexes. These trimers-of-dimers are thus a key stage in the formation of the capsid structure [28,33]. It appears that the trimers may join to the existing feature from various points, therefore growth is multi-directional. On both single and mixed phase bilayers, self-assembly was observed, with similar complexes being formed to different extents. However, the sizes of the nucleation complexes observed on a mixed bilayer (Fig. 4D-F) were larger than those observed on single phase bilayers. Thus phase separation, or the diversity of the lipids, may increase the rate of structure assembly.

Following these results previously proposed models for in-vitro self-assembly[20] of the HIV capsid can be expanded to include information on the nucleation complexes (Fig. 5). Unlike previously proposed models, these experiments were carried out at low salt concentrations (0.1M NaCl), yet the structures formed measured were very similar in width (previous = 54 ± 8 nm compared with 62.6 ± 2.85 nm (DOPC) and 50.0 ± 0.61 nm (DPPC)). The stepwise assembly of the "curling tadpole" is consistent with the data on both lipid surfaces whereby characteristic structures at each stage of the model are apparent

Single molecule force spectroscopy using a CA protein functionalised tip was used to measure the strength of interaction between the CA protein and each of the component lipids in the phase separated bilayers. Forced unfolding of the protein was seen to generate saw-tooth patterns (Fig. 6B). The protein is able to both bind and unfold in various orientations thus generating different degrees of saw-tooth. The detachment force required to pull the molecule of the surface of interest was measured (Fig. 6C-D), with measurements also being taken on mica to provide a reference value (Fig. 6A). The force required to pull the protein of the DOPC fluid phase was found to be significantly higher than that required to detach from the DPPC gel phase or even on bare mica. It is difficult to relate this difference to assembly mechanism. However it is clear that there is a differential adhesion force in the mixed bilayer as opposed to single component, which could be related to the differences in capsid assembly observed for the two systems.

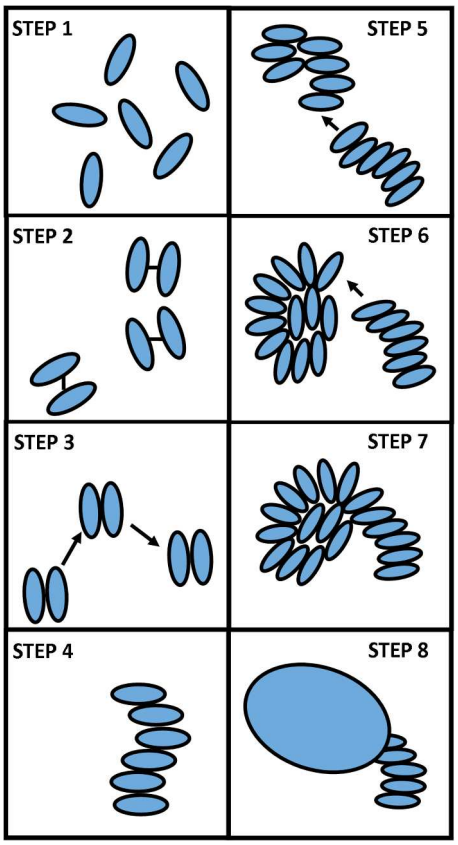

Fig 5. HIV capsid *in-vitro* assembly model. Individual CA proteins associate to form stable dimers in solution, which are able to move through the bilayer, the movement of these dimers is rate limiting. The dimers associate to form trimers-of-dimers; these are seen as curved chains of six proteins. These chain then coil up to form larger structures, dimers appear to associate into chains close to the larger structures. More chains add on to the end of the feature to increase its size. Whilst the model shows that the chains only join from one point on the feature, it appears that this growth can occur at both ends of the feature.

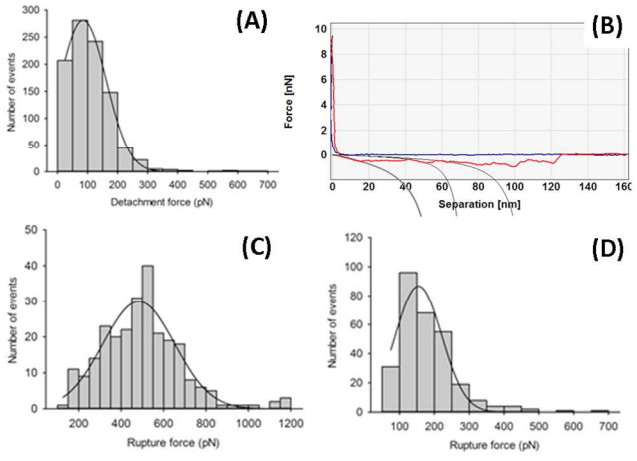

Fig 6. Single molecule force spectroscopy analysis. Gold cantilever tips were functionalized with CA for 60 minutes. Force spectroscopy was carried out on mica (A), DOPC fluid phase domains (C) and DPPC del phase domains (D). A representative force spectrum which exhibits a saw tooth pattern, indicating unfolding of the CA molecule can be fitted to the worm-like chain model (B).

Table 1 'Tadpole' feature dimensions. A tadpole feature on a DOPC bilayer was monitored over a 20 minute period (Fig 2C.) the dimensions of the 'tadpole' head and tail were measured at 10 minute intervals. After 20 minutes, there was little growth observed due to the limited availability of CA molecules.

Time (min)	0	10	20
Length (nm)	148	189	194
Width (nm)	113	118	126
Tail Length (nm)	150	267	2323

Conclusions

When adsorbed onto a mica surface, CA protein is seen to exist as either single molecules or dimers, over time there is no significant change in the feature sizes. Upon adsorbtion onto lipid bilayers, a range of structures are observed which can be categorised as either nucleation or growth complexes. On phase separated bilayers consisting of two components, the CA protein gains mobility and is able to assemble with ease, in the process disrupting the gel phase domains. Chain like features assemble that eventually wind into a capsid like structure. The use of atomic force microscopy to follow this process has allowed us to follow assembly at molecular resolution. Even though time lapse imaging of individual capsid assembly is only possible in isolated cases, multiple examples of each stage of assembly are apparent over the bilayer surface allowing a number of stages in capsid protein assembly to be observed. Of fundamental significance is the relative ease of assembly of the protein on lipid bilayers as opposed to mica. In this sense the lipid bilayer acts as a crowding agent and promotes protein assembly. Thus this work suggests that membrane P24 interactions may indeed be a factor in capsid assembly.

Acknowledgements

Dr Lynn Donlon is gratefully acknowledged for technical support.

Notes and references

a Chemical Engineering and Advanced Materials, Newcastle University, Newcastle Upon Tyne.
** Chemical Engineering and Advanced Materials, Newcastle University, Newcastle Upon Tyne, NE1 7RU.; E-mail: d.j.frankel@newcastle.ac.uk*

1. Barresinoussi F, Chermann JC, Rey F, Nugeyre MT, Chamaret S, Gruest J, et al. Science. 1983;220(4599):868-71.
2. Wasik BR, Turner PE. Annu Rev Microbiol. 2013;67:519-41.
3. Walker BD, Burton DR. Science. 2008;320(5877):760-4.
4. Carrington M, Alter G. Csh Perspect Med. 2012;2(7).
5. Engelman A, Cherepanov P. Nat Rev Microbiol. 2012;10(4):279-90.
6. Klumpp K, Crepin T. Curr Opin Virol. 2014;5:63-71.
7. Ganser-Pornillos BK, Yeager M, Sundquist WI. Curr Opin Struc Biol. 2008;18(2):203-17.
8. Wilk T, Gross I, Gowen BE, Rutten T, de Haas F, Welker R, et al. J Virol. 2001;75(2):759-71.
9. Fuller SD, Wilk T, Gowen BE, Krausslich HG, Vogt VM. Curr Biol. 1997;7(10):729-38.
10. Briggs JAG, Simon MN, Gross I, Krausslich HG, Fuller SD, Vogt VM, et al. Nat Struct Mol Biol. 2004;11(7):672-5.
11. Barklis E, McDermott J, Wilkens S, Fuller S, Thompson D. J Biol Chem. 1998;273(13):7177-80.
12. Barklis E, Alfadhli A, McQuaw C, Yalamuri S, Still A, Barklis RL, et al. J Mol Biol. 2009;387(2):376-89.
13. del Alamo M, Rivas G, Mateu MG. J Virol. 2005;79(22):14271-81.
14. Deshmukh L, Schwieters CD, Grishaev A, Ghirlando R, Baber JL, Clore GM. Journal of the American Chemical Society. 2013;135(43):16133-47.
15. Ehrlich LS, Liu TB, Scarlata S, Chu B, Carter CA. Biophys J. 2001;81(1):586-94.
16. Gamble TR, Vajdos FF, Yoo SH, Worthylake DK, Houseweart M, Sundquist WI, et al. Cell. 1996;87(7):1285-94.
17. Gamble TR, Yoo SH, Vajdos FF, vonSchwedler UK, Worthylake DK, Wang H, et al. Science. 1997;278(5339):849-53.
18. Berthet-Colominas C, Monaco S, Novelli A, Sibai G, Mallet F, Cusack S. Embo J. 1999;18(5):1124-36.
19. Pornillos O, Ganser-Pornillos BK, Yeager M. Nature. 2011;469(7330):424-+.
20. Ehrlich LS, Agresta BE, Carter CA. J Virol. 1992;66(8):4874-83.
21. Benjamin J, Ganser-Pornillos BK, Tivol WF, Sundquist WI, Jensen GJ. J Mol Biol. 2005;346(2):577-88.
22. Ganser BK, Li S, Klishko VY, Finch JT, Sundquist WI. Science. 1999;283(5398):80-3.
23. Zhao GP, Perilla JR, Yufenyuy EL, Meng X, Chen B, Ning JY, et al. Nature. 2013;497(7451):643-6.
24. Ganser-Pornillos BK, von Schwedler UK, Stray KM, Aiken C, Sundquist WI. J Virol. 2004;78(5):2545-52.
25. Briggs JAG, Wilk T, Welker R, Krausslich HG, Fuller SD. Embo J. 2003;22(7):1707-15.
26. Campbell S, Vogt VM. J Virol. 1995;69(10):6487-97.
27. Briggs JAG, Gruenewald K, Glass B, Foerster F, Kraeusslich HG, Fuller SD. Structure. 2006;14(1):15-20.
28. Grime JMA, Voth GA. Biophys J. 2012;103(8):1774-83.
29. Leonenko ZV, Cramb DT. Nato Sci Ser Ii Math. 2005;186:475-+.
30. Singer SJ, Nicolson GL. Science. 1972;175(4023):720-&.
31. Simons K, Ikonen E. Nature. 1997;387(6633):569-72.
32. Ganser-Pornillos BK, Cheng A, Yeager M. Cell. 2007;131(1):70-9.
33. Chen B, Tycko R. Biophys J. 2011;100(12):3035-3044.

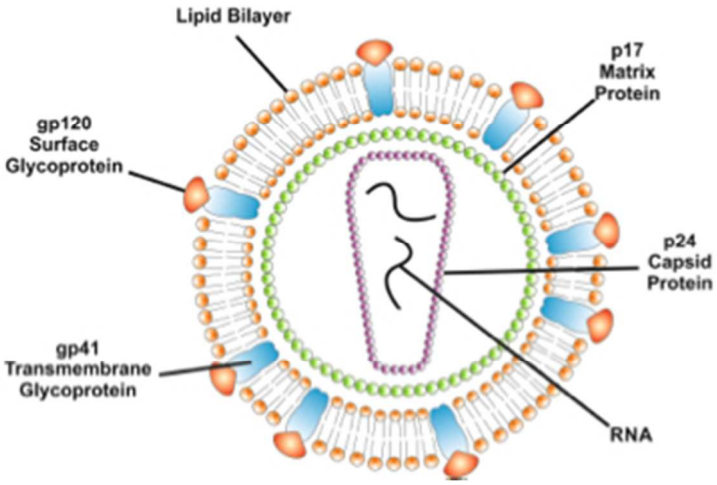

Curling tadpole mechanism of viral capsid assembly